RESULTS FROM STAR BEAM ENERGY SCAN PROGRAM*

Michal Šumbera

for the STAR Collaboration

Nuclear Physics Institute ASCR, 250 68 Řež, Czech Republic

(Received January 25, 2013)

Results from the Beam Energy Scan (BES) program conducted recently by STAR experiment at the RHIC are presented. The data from Phase-I of the BES program collected in Au+Au collisions at center-of-mass energies ($\sqrt{s_{NN}}$) of 7.7, 11.5, 19.6, 27, and 39 GeV cover a wide range of baryon chemical potential μ_B (100–400 MeV) in the QCD phase diagram. Results from the BES Phase-I related to the "turn-off" of strongly interacting quark-gluon plasma (sQGP) signatures and signals of QCD phase boundary are reported. In addition to this, an outlook is presented for the future BES Phase-II program and a possible fixed target program at STAR.

DOI:10.5506/APhysPolBSupp.6.429
PACS numbers: 25.75.Ld, 25.75.Nq

1. Introduction

At sufficiently high temperature T or baryon chemical potential μ_B, QCD predicts a phase transition from hadrons to the plasma of its fundamental constituents — quarks and gluons [1]. Search for and understanding of the nature of this transition has been a long-standing challenge to high-energy nuclear and particle physics community. In 2005, just five years after start up of RHIC, the first convincing arguments on the existence of de-confined strongly interacting partonic matter with unexpected properties of perfect quark-gluon liquid, constituent number scaling, jet quenching and heavy-quark suppression were revealed [2]. A central goal now is to map out as much of the QCD phase diagram in T, μ_B plane as possible, trying to understand various ways in which the hadron-to-sQGP transition may occur. STAR proposal for the BES program was published in 2010 [3]. The goal

* Presented at the International Symposium on Multiparticle Dynamics, Kielce, Poland, September 17–21, 2012.

is to search for the "turn-off" of sQGP signatures, signals of QCD phase boundary and existence of a critical point in the QCD phase diagram. First two topics are covered in this paper, the last one is discussed in two other STAR contributions to this conference [4, 5].

The results presented here are based on the data collected by the STAR Collaboration. The almost uniform acceptance for different identified particles and collision energies at midrapidity is an important advantage of the STAR detector for the BES program. The main tracking device — the Time Projection Chamber (TPC) — covering 2π in azimuth (ϕ) and -1 to 1 in pseudorapidity (η) provides momentum measurements as well as particle identification (PID) of charged particles. For the higher transverse momentum (p_{T}) region, the Time-Of-Flight (TOF) detector is quite effective in distinguishing between different particle types. Particles are identified using the ionization energy loss in TPC and time-of-flight information from TOF [6]. The centrality selection in STAR is done using the uncorrected charge particle multiplicity measured in the TPC within $|\eta| < 0.5$ [7].

During its twelve years of operation, the RHIC machine has delivered a variety of nuclear beams (Au, Cu, d). The most frequently used c.m.s. energies per nucleon–nucleon pair were $\sqrt{s_{NN}} = 200$ and 62.4 GeV. The last few years have witnessed, quite naturally, a shift of experimental activity to lower energies as well as a change of the colliding species. After few small-statistic, Cu+Cu exploration runs at $\sqrt{s_{NN}} = 22.4$ GeV in 2005 and with Au+Au at $\sqrt{s_{NN}} = 9.2$ GeV in 2008 [7], STAR collected large-statistics data sets with Au+Au at $\sqrt{s_{NN}} = 7.7$, 11.5 and 39 GeV in 2010, and 19.6 and 27 GeV in 2011 [8]. It is noteworthy that $\sqrt{s_{NN}} = 7.7$ GeV, which is much below the RHIC design injection energy of 19.6 GeV, remains, so far, also the lowest energy achieved with hadron collider. In 2012, RHIC collided

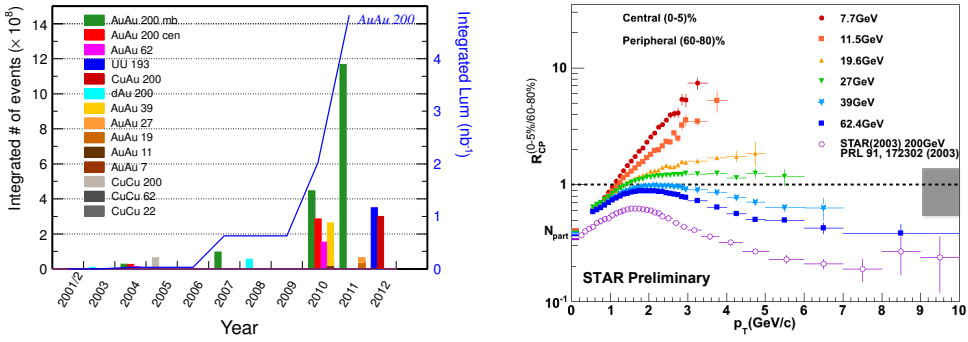

Fig. 1. Left panel: Heavy-ion minimum bias/central data sets (histograms) and integrated luminosity (line) recorded by the STAR detector. Right panel: $R_{\mathrm{CP}}^{(0-5\%/60-80\%)}$ for charged hadrons in Au+Au collisions at $\sqrt{s_{NN}} = 7.7$–39 GeV. Errors are statistical only. Grey band represents the normalization error from N_{bin}.

for the first time two uranium beams at $\sqrt{s_{NN}} = 193$ GeV. The left panel of Fig. 1 shows the statistics of the recorded heavy-ion data from all RHIC runs by the STAR detector. Significant amounts of data have been accumulated since 2010 when the fast data acquisition and the TOF subsystem upgrades were completed.

2. "Turn-off" of sQGP signatures

2.1. Suppression of high-p_{T} hadrons

Important signature of sQGP at top RHIC energy is the Nuclear Modification Factor R_{CP} [2], which is defined as ratio of yields at central collisions to peripheral collisions, scaled by the corresponding number of binary collisions N_{bin}. It has been observed that at high p_{T}, the R_{CP} of different particles is less than unity [2], which is attributed to the energy loss of the partons in the dense sQGP medium. In the absence of dense medium, there may not be suppression of high p_{T} particles.

The right panel of Fig. 1 shows the R_{CP} of charged hadrons in Au+Au collisions at $\sqrt{s_{NN}} = 7.7$–200 GeV. We observe that for $p_{\mathrm{T}} > 2$ GeV/c, the R_{CP} is less than unity at 39 GeV and then, the value increases as the beam energy decreases. For $\sqrt{s_{NN}} > 27$ GeV, R_{CP} is below unity, indicating a dominant role of partonic effects. Another interesting pattern is provided by the energy dependence of R_{CP} of various strange hadrons such as K^0_{S}, ϕ, Λ, Ξ^-, and Ω^-. First, baryon–meson splitting observed at top RHIC energy reduces and disappears with decreasing energy. Second, for $p_{\mathrm{T}} > 2$ GeV/c, the $R_{\mathrm{CP}}(K^0_{\mathrm{S}})$ is less than unity at 39 GeV and then, the value increases as the beam energy decreases. For $\sqrt{s_{NN}} < 19.6$ GeV, $R_{\mathrm{CP}}(K^0_{\mathrm{S}})$ is above unity, indicating decreasing partonic effects at lower energies. For more information on identified hadrons results, see [8].

2.2. Elliptic flow

Study of the conversion of coordinate space anisotropies into momentum space anisotropies plays a central role in ongoing efforts to characterize the transport properties of sQGP. The azimuthal anisotropic flow strength is usually parametrized via Fourier coefficients $v_n \equiv \langle \cos[n(\phi - \Psi)] \rangle$, where ϕ is the azimuthal angle of the particle and Ψ is the azimuthal angle of the event plane (EP). The big surprise at RHIC came from the measurement of the v_2 coefficient, integrated elliptic flow, which brings information on the pressure and stiffness of the equation of state during the earliest collision stages. It was found that v_2 increases by 50% from the top SPS energy $\sqrt{s_{NN}} = 17.2$ GeV to the top RHIC energy $\sqrt{s_{NN}} = 200$ GeV [2]. The large value of v_2 observed at RHIC and later on at LHC [9] is one of the cornerstones of the perfect liquid bulk matter dynamics. Moreover, the differential

$v_2(p_T)$, that characterizes the hydrodynamic response to the initial geometry, seems to be unchanged between the top RHIC energy and LHC energy of $\sqrt{s_{NN}} = 2.76$ TeV [9]. Recently published data from STAR utilizing instead of previously used η sub-event method $v_2\{\text{EtaSubs}\}$, another elliptic flow method, 4-particle cumulants $v_2\{4\}$, slightly modify this picture [10]. Advantage of the cumulant method is that it removes the contribution of non-flow correlations. Systematic study of centrality, transverse momentum and pseudorapidity dependence of the inclusive charged hadron elliptic flow $v_2\{4\}$ at midrapidity has shown that, as the collision energy varies from $\sqrt{s_{NN}} = 7.7$ to 2760 GeV, the experimental data at all energies do not reveal an exact scaling. They show larger splitting in the lower p_T region and converge at the intermediate range ($p_T \sim 2$ GeV/c). The increase of $v_2(p_T)$ with $\sqrt{s_{NN}}$ could be due to the change of chemical composition from low to high energies and/or larger collectivity at the higher collision energy.

STAR BES results [11, 12] on v_2 of identified particles in the regime where the relative contribution of baryon and mesons vary significantly are presented in Fig. 2. In the left panel, the difference in v_2 between particles (X) and their corresponding anti-particles ($\overline{X}$) is plotted. A beam-energy dependent difference of the values of v_2 between particles and corresponding anti-particles increases with decreasing beam energy and is larger for baryons compared to mesons. Interestingly, the flow patterns are also reflected in the number-of-constituent-quarks (NCQ) scaling of particle identified data. Plotting v_2/n_q *versus* $(m_T - m_0)/n_q$ for various particle species, where n_q is

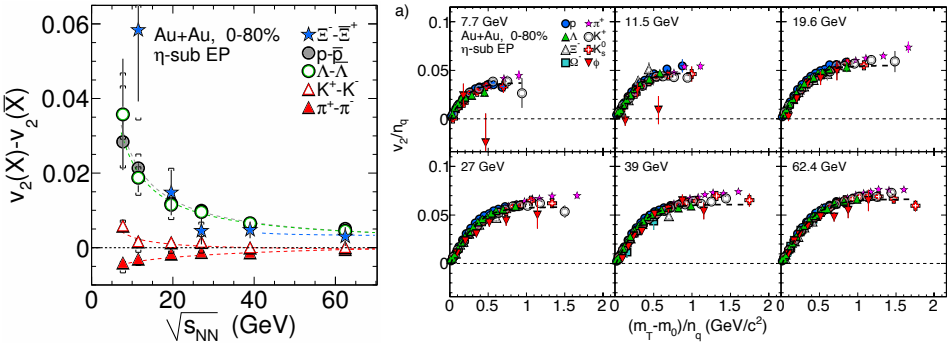

Fig. 2. (Color online) Left panel: The difference in v_2 between particles (X) and their corresponding anti-particles ($\overline{X}$) as a function of $\sqrt{s_{NN}}$ for 0–80% central Au+Au collisions [11]. The dashed lines in the plot are fits with a power-law function. The error bars depict the combined statistical and systematic errors. Systematic errors are plotted by caps, not combined in the error bars. Right panel: v_2/n_q *versus* $(m_T - m_0)/n_q$, for 0–80% central Au+Au collisions for selected particles [12].

the number of constituent quarks of a hadron with mass m_0 and $m_T - m_0$ is its transverse kinetic energy, one finds the data at $\sqrt{s_{NN}} = 200$ GeV to collapse onto a single universal curve [2]. The observed beam-energy difference between particles and anti-particles implies that, at lower energies, particles and anti-particles are not consistent with the universal NCQ scaling of v_2. Such a breaking of the NCQ scaling could indicate increased contributions from hadronic interactions in the system evolution with decreasing beam energy. Nevertheless, for each given energy particles (see the right panel of Fig. 2) appear to follow the scaling. Note that the v_2 values for ϕ mesons at 7.7 and 11.5 GeV are approximately two standard deviations away from the trend defined by the other hadrons at the highest measured p_T values.

2.3. Charge separation with respect to the reaction plane

The concept of Local Parity ($\mathcal{P}$) Violation (LPV) in high-energy heavy ion collisions was first brought up by Lee [13] and elaborated by Kharzeev *et al.* [14]. In non-central collisions, such a $\mathcal{P}$-odd domain can manifest itself via preferential the same charge particle emission for particles moving along the system's angular momentum, due to the Chiral Magnetic Effect (CME) [15]. To study this effect, a three-point mixed harmonics azimuthal correlator $\gamma = \langle \cos(\phi_\alpha + \phi_\beta - 2\psi_{RP}) \rangle$ was proposed [16]. Here, ϕ is the particle azimuthal angle, α and β denote the particle type: α, $\beta = +, -$ and ψ_{RP} is the reaction plane azimuth. The observable γ is $\mathcal{P}$-even, but sensitive to the fluctuation of charge separation. STAR measurements of the correlator were reported for Au+Au and Cu+Cu collisions at 200 GeV

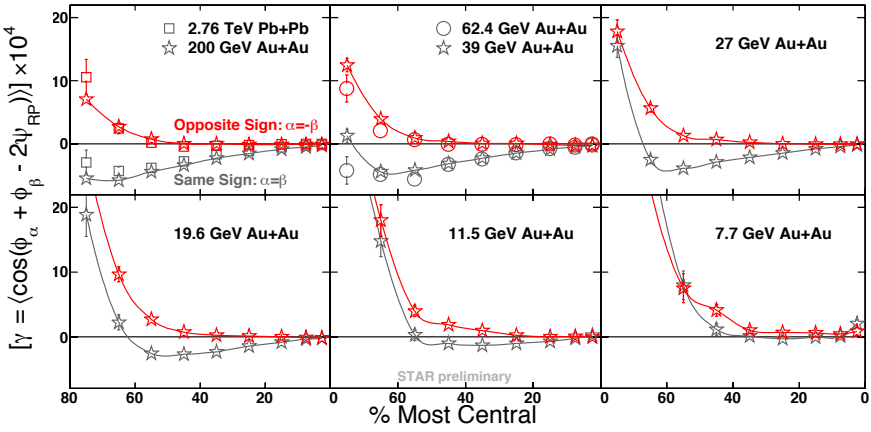

Fig. 3. (Color online) The three-point correlator, γ, as a function of centrality for Au+Au collisions from 200 GeV to 7.7 GeV [19]. For comparison, we also show the results for Pb+Pb collisions at 2.76 TeV [20]. The errors are statistical only.

and 62.4 GeV [17, 18], showing a clear difference between the opposite sign (OS) and the same sign (SS) correlations, qualitatively consistent with the picture of CME and LPV. Fig. 3 presents the extension of the analysis to lower beam energies. The results for Pb+Pb collisions at 2.76 TeV [20] are also shown for comparison purposes. A striking similarity exists between 2.76 TeV and 200 GeV data. With further decrease in $\sqrt{s_{NN}}$ a smooth transition occurs starting from the peripheral collisions. At 7.7 GeV the difference between OS and SS signal disappears.

3. Signals of QCD phase boundary

In non-central heavy ion collisions, initial eccentricity of the participant zone in the transverse plane leads to an out-of-plane extended ellipsoid. At higher energies, one expects stronger pressure gradients, which would cause the shape to become more spherical. Systems with a longer lifetime, as well, would achieve a more spherical shape or could even conceivably become extended in-plane [22]. Based on these two considerations, we would expect the excitation function for the freeze-out eccentricity to fall monotonically with increasing energy. The excitation function of the freeze-out eccentricity ε_{f} for a centrality of 10–30% and rapidity ranges of $[-0.5, 0.5]$, $[-1, -0.5]$ and [0.5,1] in Au+Au collisions are given in Fig. 4 as a function of $\sqrt{s_{NN}}$. The STAR measurements are consistent with a monotonically decreasing trend. Comparison to models [23] shows that the prediction from UrQMD comes closest to describe the measurements from STAR and AGS simultaneously. The hybrid models tend to come close to the CERES point [24] but underpredict the rest, while 2D hydrodynamic predictions tend to overpredict the data at most energies.

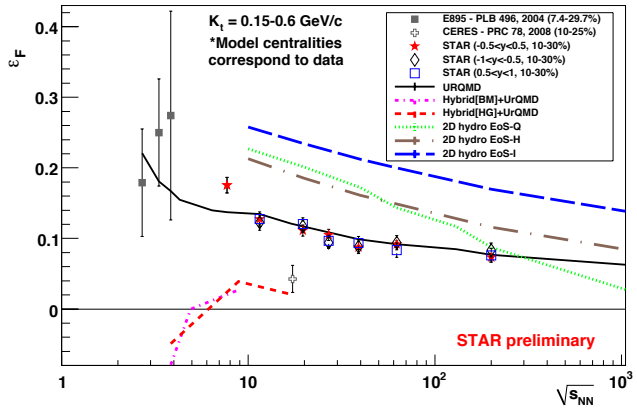

Fig. 4. (Color online) Freeze-out eccentricity, ε_{f}, as a function of $\sqrt{s_{NN}}$ for data and models [21].

4. The BES Phase-II and STAR in fixed target mode

To strengthen the message from Phase-I, higher statistics at lower energies is needed, especially at 7.7 and 11.5 GeV. Statistics for several important observables, such as ϕ-meson v_2 or higher moments of net-protons distributions [5], are not sufficient to draw quantitative conclusions. In order to confirm the trends between 11.5 and 19.6 GeV, another energy point is needed around 15 GeV in order to fill the 100 MeV gap in μ_B. This will be a part of the BES Phase-II program proposed by STAR. Simulation results indicate that with electron cooling, the luminosity could be increased by a factor of about 3–5 at 7.7 GeV and about 10 around 20 GeV [26]. The request for an electron cooling device at RHIC has already been submitted by STAR. An additional improvement in luminosity may be possible by operating with longer bunches at the space-charge limit in the collider [27]. Altogether a factor or 10 improvement in luminosity is expected after these modifications. This will not only allow the precision measurements of the above important observables but will also help in the measurements of rare probes such as dileptons and hypertritons.

To maximize the use of collisions provided by RHIC for the BES program, an option to run STAR as a fixed-target experiment is under consideration. A fixed Au target is to be installed in the beam pipe. This will allow the extension of the μ_B range from 400 MeV to about 800 MeV covering thus a substantial portion of the phase diagram. The data taking can be done concurrently during the normal RHIC running. This proposal will not affect the normal RHIC operations. The following table lists the proposed collision energies, corresponding fixed target center-of-mass energies, and baryon chemical potential values. The μ_B values are listed for the central collisions corresponding to fixed target [25].

Collider mode $\sqrt{s_{NN}}$ [GeV]	Fixed-target mode $\sqrt{s_{NN}}$ [GeV]	μ_B [MeV]
19.6	4.5	585
15	4.0	625
11.5	3.5	670
7.7	3.0	720
5	2.5	775

5. Summary

Recent results from Phase-I of the RHIC BES program have substantially extended our knowledge of hot and dense de-confined QCD matter. Interesting but smooth patterns of energy dependence are seen in most of the presented analyses. Significant differences in particle and anti-particle

v_2 coming from the high net-baryon density show up at midrapidity. This indicates increased contributions from hadronic interactions in the system evolution with decreasing beam energy.

This work was supported by grant LA09013 of the Ministry of Education of the Czech Republic.

REFERENCES

[1] Y. Aoki *et al.*, *Nature* **443**, 675 (2006).
[2] J. Adams *et al.* [STAR Coll.], *Nucl. Phys.* **A757**, 28 (2005).
[3] M.M. Aggarwal *et al.* [STAR Coll.], `arXiv:1007.2613 [nucl-ex]`.
[4] N.R. Sahoo [STAR Coll.], *Acta Phys. Pol. B Proc. Suppl.* **6**, 437 (2013), this issue.
[5] Z. Li [STAR Coll.], *Acta Phys. Pol. B Proc. Suppl.* **6**, 445 (2013), this issue.
[6] M. Anderson *et al.*, *Nucl. Instrum. Methods* **A499**, 659 (2003); W. Llope, *Nucl. Instrum. Methods* **A661**, S110 (2012).
[7] B.I. Abelev *et al.* [STAR Coll.], *Phys. Rev.* **C81**, 024911 (2010).
[8] L. Kumar [STAR Coll.], `arXiv:1211.1350 [nucl-ex]`.
[9] K. Aamodt *et al.* [ALICE Coll.], *Phys. Rev. Lett.* **105**, 252302 (2010).
[10] L. Adamczyk *et al.* [STAR Coll.], *Phys. Rev.* **C86**, 054908 (2012).
[11] L. Adamczyk *et al.* [STAR Coll.], `arXiv:1301.2347 [nucl-ex]`.
[12] L. Adamczyk *et al.* [STAR Coll.], `arXiv:1301.2348 [nucl-ex]`.
[13] T.D. Lee, *Phys. Rev.* **D8**, 1226 (1973).
[14] D. Kharzeev, R.D. Pisarski, M.H.G. Tytgat, *Phys. Rev. Lett.* **81**, 512 (1998).
[15] D. Kharzeev, *Phys. Lett.* **B633**, 260 (2006).
[16] S.A. Voloshin, *Phys. Rev.* **C70**, 057901 (2004).
[17] B.I. Abelev *et al.* [STAR Coll.], *Phys. Rev. Lett.* **103**, 251601 (2009).
[18] B.I. Abelev *et al.* [STAR Coll.], *Phys. Rev.* **C81**, 054908 (2010).
[19] D. Gangadharan *et al.* [STAR Coll.], *J. Phys. G* **38**, 124166 (2011).
[20] B. Abelev *et al.* [ALICE Coll.], *Phys. Rev. Lett.* **110**, 012301 (2013).
[21] N. Shah [STAR Coll.], `arXiv:1210.5436 [nucl-ex]`.
[22] P.F. Kolb, U.W. Heinz, `arXiv:nucl-th/0305084`.
[23] M. Lisa *et al.*, *New J. Phys.* **13**, 065006 (2011).
[24] D. Adamová *et al.* [CERES Coll.], *Phys. Rev.* **C78**, 064901 (2008).
[25] J. Cleymans *et al.*, *Phys. Rev.* **C73**, 034905 (2006).
[26] A. Fedotov, W. Fischer, private communications, 2012.
[27] A. Fedotov, M. Blaskiewicz, BNL CAD Tech Note: C-A/AP/449 (February 10, 2012).